

Novel Use of Synthetic Aperture Technique to Improve Image Quality in Ultrasound Elastography: Preliminary Investigation

Arpan Ghosh

Department of Applied mechanics and Biomedical Engineering
Indian Institute of Technology Madras
Chennai, India
am20s036@smail.iitm.ac.in

Dr. Arun Kumar Thittai

Department of Applied mechanics and Biomedical Engineering
Indian Institute of Technology Madras
Chennai, India
akthittai@iitm.ac.in

Abstract—Quasi-static elastography (QSE) is a well-known technique, where the ultrasound data acquired before and after a small tissue compression is analyzed to form an image, which is related to the stiffness parameter of the underlying tissue. Most studies have reported the effect of Conventional Focused Beamforming (CFB) transmit scheme on image quality of ultrasound elastography. Recently, Diverging Beam Synthetic Aperture technique (DBSAT) has been shown to improve the image quality of ultrasound images, however, very little is explored of this scheme for elastography application. This research paper presents a novel strategy to obtain better quality elastography images using the DBSAT transmit scheme. The widely used CFB technique is a line-by-line scanning technique that produces one elastogram by processing one pre-compression and one post-compression frame, however, DBSAT being a synthetic aperture approach produces several low-resolution images before summing to obtain one high resolution image. In this experimental work on tissue-mimicking phantom, we demonstrate that estimating 128 low resolution elastograms and summing them to produce one high resolution elastogram is an effective way to reduce noise and increase the elastographic image quality. More than 15dB improvement was found when comparing the image quality metrics of signal-to-noise ratio (SNR) and Contrast-to-noise ratio (CNR) from elastography images obtained from DBSAT vs. that obtained from CFB scheme.

Keywords—*Ultrasound, Beamform, Elastogram, CFB, DBSAT, RF.*

I. INTRODUCTION

In the last decade, elastography has found its way as an offered option in most of the commercial ultrasound scanners. There are two techniques available, which are (i) Shear wave based elastography and (ii) Quasi-static elastography. Shear wave based elastography has been extensively used in ultrasound device for liver imaging application. Quasi-static elastography, which is also sometimes referred to as real time elastography is also popular for clinical application [1]. The advantages of quasistatic elastography are (i) this mode is feasible in basic diagnostic ultrasound scanner and (ii) the tissue elasticity measurement is in real time. The disadvantage of using this technique is that it is not quantitative in nature [2]. The governing principle behind elastography is that when a tissue is deformed by applying stress, the resultant strain can

be estimated to obtain the underlying tissue stiffness. Stiffer regions will experience smaller strain compared to softer regions that will experience larger strain. The image of the strain distribution map of a medium is known as elastogram [1]. This strain generated in a medium can be axial strain or lateral strain depending on the deformation direction. In addition to the strains, any rigid body rotation can also be estimated by combining the axial and lateral shear strain components, and this is referred to as rotational elastogram [4].

Tissue elasticity mimicking phantoms are used in various research studies serve as an artificial representation of real biological tissues. Typically, stress is applied on the phantom to induce deformation in the axial direction. There are two common methods to apply stress (i) free-hand compression or (ii) controlled compression. In the existing body of literature, agar-gelatin tissue-mimicking phantom is used in the experimental works reported [3]. In addition to understand the fundamentals of elastography in terms of theory of elasticity, we have to consider the ultrasound signal processing schemes, which are well described by Lokesh et.al [4].

In literature, it is shown that the choice of ultrasound data acquisition transmit techniques along with signal processing schemes together significantly influences the quality of elastograms. Therefore, to image a medium using ultrasound modality, there are several transmit schemes that can be employed. Conventional focused beam (CFB) technique is a well-established transmit scheme, which has been extensively used. Recently, diverging beam synthetic aperture (DBSAT) scheme was introduced as a better alternative to CFB [4]. The drawback of CFB is that the lateral resolution in the image deteriorates as we move away from the focus, due to the shape of the beam (hourglass shaped). Whereas, using DBSAT good lateral resolution can be obtained throughout the depth of imaging [4][5]. In addition, DBSAT scheme provides an image frame in every transmit as opposed to only one A-line in the case of CFB, therefore providing an opportunity to exploit the potential of higher framerate (10's of times) to track finer tissue motions. The data collected by these transmit schemes are RF data (radio frequency), which is beamformed in the ultrasound scanner. This beamformed RF data is processed further in a 2D displacement tracking algorithm [6] to get axial strain elastograms (ASE). For most of the work in elastography, the elastograms are obtained by choosing pre- and post-

compression frames separated by a predetermined compressive strain.

In literature, a comprehensive analysis of using dynamic frame pairing method in freehand elastography incorporating CFB transmit scheme is reported [7]. In some studies it is demonstrated that the strain estimates obtained by averaging reduce the standard deviation of the averaged elastogram by \sqrt{N} (where N is the number of frames), thereby, improving the SNR of the elastogram by the same factor [8] [9]. It is shown that the rate at which SNR decreases is smaller for small strain increments. There is a relation between multi-compression averaging and image quality, captured using the strain filter [12]. Therefore, all the elastograms are generated by deforming the medium within 1~3 % of its axial dimension. Literature also reports another well-established concept of temporal stretching, and how it leads to an improvement in SNR over a wider range of applied strains [11] [14].

The primary focus of this research paper is to explore the use of the low-resolution frame data, obtained using the DBSAT technique, for generating higher quality elastograms. Here, we aimed to obtain a high resolution elastogram frame by averaging all the elastograms obtained from low resolution frames. This novel approach by tapping into the low resolution frames to exploit the unique advantage of the synthetic aperture technique has not been investigated in literature to the best of our knowledge.

II. MATERIALS AND METHODS

A. Phantom Preparation

Experimental studies were performed on agar-gelatin tissue-mimicking phantom. The phantom had dimensions of $70 \times 70 \times 70$ mm (height \times width \times length) with two circular cylindrical inclusions of 70×30 mm and 70×20 mm (length \times diameter) at depths of 25mm and 60mm.

Two solutions were prepared, one containing 5% by weight gelatine and 3% by weight agar in 500 ml of de-ionized water and another containing 3% by weight agar and 15% by weight gelatine in 500 ml of de-ionized water. First, the background of the phantom was prepared by pouring the 5% gelatine solution in the mould and allowing it to set. Afterwards two circular gaps were created in the background and inclusion material having 15% gelatine was poured into them to create the targets.

Apart from the above, one homogeneous phantom was prepared for SNR analysis that had dimensions of $70 \times 70 \times 70$ mm (height \times width \times length) with the 5% by weight gelatine and 3% by weight agar composition.

B. Data Acquisition

The data was acquired using DBSAT and CFB transmit schemes with 128 element linear array transducer. RF data was collected using ultrasound research scanner (Vantage 64, Verasonics, WA, USA). The transducer was operated with a center frequency of 7.8 MHz with a sampling frequency of 41.2 MHz. In DBSAT imaging active aperture of 8 elements was used to send a diverging beam into the medium, whereas in CFB, active aperture of 64 elements was used. The beam was focused at 25 mm in axial direction. The transducer was

attached to a compressor plate which was attached to a digital motion controller. First experiment was done on the two-inclusion phantom which was submerged in water and deformed by 1.6% in the axial direction. The pre-compression and post-compression RF data were collected with both transmit schemes. The data was exported from the scanner and processed with delay and sum (DAS) algorithm to form beamformed RF data.

Afterwards second experiment was done on a homogeneous phantom. Where pre-compression and post-compression RF data were collected simultaneously for each small incremental strain value applied on the phantom. The maximum deformation subjected on the phantom was 4.5% in the axial direction.

C. Displacement Estimation

The tissue displacement was estimated by 2D multilevel displacement tracking algorithm. The beamformed RF data was processed by feeding the data through three levels of displacement tracking. The final axial displacement estimate was used to generate the ASE. The axial window size used in coarse 1, coarse 2 and fine level were 25λ , 5λ , 3λ and the lateral window size kept as 0.6mm. The detailed explanation of search window length settings and window sizes are reported [6]. The entire flow of the data processing using DBSAT transmit scheme is shown in the Fig. 1

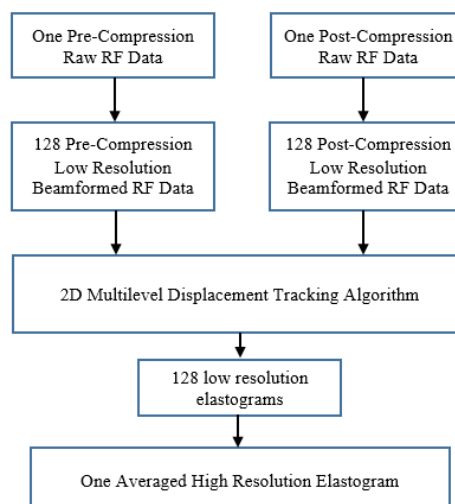


Fig.1 Block diagram of the entire data processing flow using DBSAT transmit scheme.

III. RESULT

To investigate the quality of elastogram the image quality parameters of signal-to-noise ratio (SNR) and Contrast-to-noise ratio (CNR) were calculated.

Fig.2 compares axial strain elastograms of the phantom acquired by CFB and DBSAT transmit schemes. It can be easily observed that the image obtained from CFB is noisy compared to DBSAT. Also in DBSAT inclusion boundaries are better defined than CFB. It is noticeable that the contrast of the inclusion at different depth showed significant improvement in the case of DBSAT. Three regions at different depths were selected to calculate contrast to noise ratio (CNR). It was calculated by taking μ (mean) and σ (standard deviation) of the corresponding inclusion and the background at different depths [4] using equation (1).

$$CNR = 20 \log_{10} \left(\frac{|\mu_{inclusion} - \mu_{background}|}{\sqrt{(\sigma_{inclusion}^2 + \sigma_{background}^2)/2}} \right) \quad (1)$$

Where, μ refers to the mean and σ refers the standard deviation.

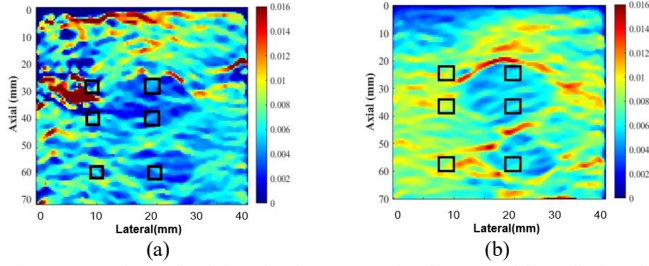


Fig.2 Comparison of axial strain elastogram of a phantom with applied strain of 1.6% acquired by CFB and DBSAT. Where (a) is one high resolution elastogram obtained by CFB and (b) is one high resolution elastogram obtained by averaging 121 low resolution elastogram using the DBSAT, for a predefined deformation. Three regions were selected to calculate CNR in different depths of the phantom which are shown as black rectangular box on the image.

Fig.3 shows the plots of SNR, CNR values computed from axial strain elastograms obtained using CFB and DBSAT schemes. The CNR values were calculated from the two-inclusion phantom which are shown in (a). Where it can be easily observed that using DBSAT provides reasonably high CNR compared to CFB scheme.

Further, the SNR values from the homogeneous phantom calculated at each incremental applied strain using equation (2) is shown in (c). It can be readily observed that the SNR value is good only in a particular range of applied strain.

$$SNR = 20 \log_{10} \left(\frac{\mu}{\sigma} \right) \quad (2)$$

Where, μ refers to the mean of the region of interest (ROI) and σ refers to the standard deviation of that corresponding ROI. The CNR values are reported in table 1.

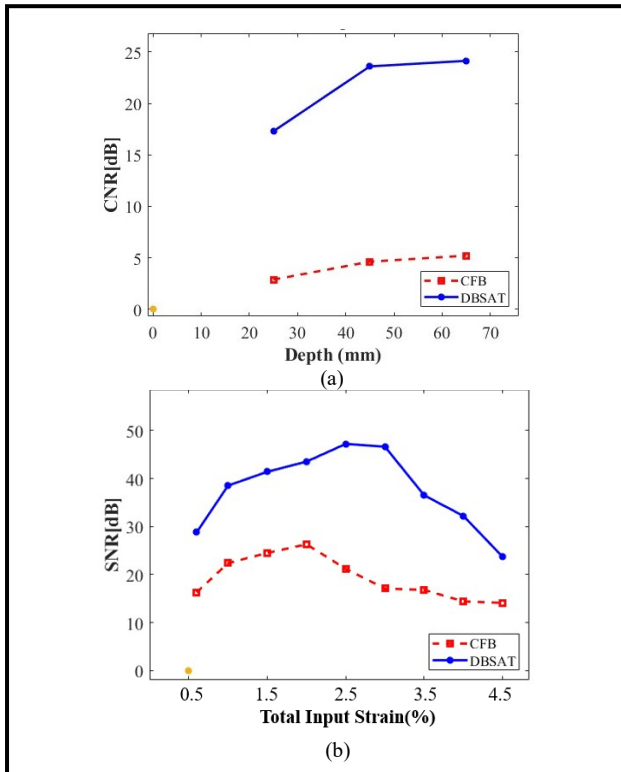


Fig.3 Plots of image quality parameters estimated from the elastograms of the two-inclusion phantom and homogeneous phantom obtained using CFB and DBSAT scheme where (a) shows CNR values in dB at depth 25mm, 45mm and 65mm. (b) shows SNR value in dB with each incremental applied strain obtained from the homogeneous phantom.

Imaging Depth(mm)	CFB	DBSAT
25	2.88	17.30
45	4.62	23.6
65	5.21	24.14

Table 1.CNR (dB)

IV. CONCLUSION

In this study, the effect of exploiting the low resolution (high frame rate) frames of DBSAT transmit scheme in ultrasound elastography was investigated. The results from Agar-Gelatin phantom illustrate that it is feasible to considerably improve the elastographic image quality compared to that obtained with CFB, by performing multi low resolution-frame averaging. Here, we report signal-to-noise ratio (SNR) and Contrast-to-noise ratio (CNR) as the preliminary analysis of image quality metrics of elastography images obtained from both CFB and DBSAT transmit scheme.

A complete analysis with multiple rendition of the experiments and statistical analysis is currently underway.

REFERENCES

- [1] Selladurai, S., Verma, A., & Thittai, A. K. (2020). Toward Quantitative and Operator-independent Quasi-static Ultrasound Elastography: An Ex Vivo Feasibility Study. *Ultrasonic Imaging*, 42(4-5), 1791-90.
- [2] Selladurai, S., & Thittai, A. K. (2019). Towards quantitative quasi-static ultrasound elastography using a reference layer for liver imaging application preliminary assessment. *Ultrasonics*, 93, 7-17.
- [3] Hall, T.J., Bilgen, M., Insana, M.F. and Krouskop, T.A., 1997. Phantom materials for elastography. *IEEE transactions on ultrasonics, ferroelectrics, and frequency control*, 44(6), pp.1355-1365
- [4] Lokesh, B., & Thittai, A. K. (2018). Diverging beam with synthetic aperture technique for Rotation elastography: preliminary experimental results. *Physics in Medicine & Biology*, 63(20), 20LT01.
- [5] Lokesh, B., & Thittai, A. K. (2019). Diverging beam transmit through limited aperture: A method to reduce ultrasound system complexity and yet obtain better image quality a higher frame rates. *Ultrasonics*, 91, 150-160
- [6] Lokesh B et al 2018 Understanding the contrast mechanism in rotation elastogram: a parametric study *Ultrasound Med. Biol.* 44 1860–72
- [7] Xia, R., Tao, G., & Thittai, A. K. (2014). Dynamic frame pairing in real-time freehand elastography. *IEEE transactions on ultrasonics, ferroelectrics, and frequency control*, 61(6), 979-985.
- [8] Varghese T, Ophir J, Céspedes I. Noise reduction in elastograms using temporal stretching with multicompression averaging. *Ultrasound Med Biol.* 1996;22(8):1043-52. doi:10.1016/s0301-5629(96)00128-7. PMID: 9004428.
- [9] Varghese T, Ophir J. Performance Optimization in Elastography: Multicompression with Temporal Stretching. *Ultrasonic Imaging* . 1996;18(3):193-214. doi:10.1177/016173469601800303
- [10] Friemel, B. H., Real-time Ultrasonic Two-dimensional Vector Velocity Estimator Utilizing Speckle-tracking Algorithm: Implementation and Irritation, Ph.D Dissertation, (Duke University, (1994). Ctspedes,
- [11] Varghese, T., and Ophir, J., A theoretical framework for performance characterization of elastography: The strain filter, *IEEE Trans. Ultrason. Ferroel. Freq. Cont.* 44, (1997)
- [12] Varghese, T., Bilgen, M., Ophir, J., and Insana, M. F., Multiresolution strain filter in elastography, Submitted to *IEEE Trans. Ultrason. Ferroel. Freq. Conr.* (1996)
- [13] Skovoroda, A. R.; Emelianov, S. Y., Lubinski, M. A., Sarvazyan, A. P., O'Donnell, M. Theoretical analysis and verification of ultrasound displacement and strain imaging, *IEEE Trans. Ultrason. Ferroel. Freq.*

Cont. 41, 302-313 (1994)

- [14] Cspedes, E. I., Insana, M. F., and Ophir, J., Theoretical bounds on strain estimation in elastography, IEEE Trans. Ultrason. Ferroel. Freq. Cont. 42, 969-972 (1995). Weinstein.